
This is an electronic reprint of the original article.
This reprint may differ from the original in pagination and typographic detail.

Stando, Grzegorz; Hannula, Pyry-Mikko; Kumanek, Bogumiła; Lundström, Mari; Janas, Dawid
Copper recovery from industrial wastewater - Synergistic electrodeposition onto nanocarbon materials

Published in:
Water Resources and Industry

DOI:
[10.1016/j.wri.2021.100156](https://doi.org/10.1016/j.wri.2021.100156)

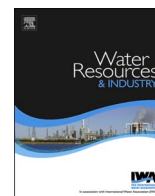
Published: 01/12/2021

Document Version
Publisher's PDF, also known as Version of record

Published under the following license:
CC BY-NC-ND

Please cite the original version:
Stando, G., Hannula, P.-M., Kumanek, B., Lundström, M., & Janas, D. (2021). Copper recovery from industrial wastewater - Synergistic electrodeposition onto nanocarbon materials. *Water Resources and Industry*, 26, Article 100156. <https://doi.org/10.1016/j.wri.2021.100156>

This material is protected by copyright and other intellectual property rights, and duplication or sale of all or part of any of the repository collections is not permitted, except that material may be duplicated by you for your research use or educational purposes in electronic or print form. You must obtain permission for any other use. Electronic or print copies may not be offered, whether for sale or otherwise to anyone who is not an authorised user.



Copper recovery from industrial wastewater - Synergistic electrodeposition onto nanocarbon materials

Grzegorz Stando^a, Pyry-Mikko Hannula^b, Bogumiła Kumanek^a, Mari Lundström^b, Dawid Janas^{a,*}

^a Department of Organic Chemistry, Bioorganic Chemistry and Biotechnology, Silesian University of Technology, B. Krzywoustego 4, 44-100, Gliwice, Poland

^b Aalto University, Department of Chemical and Metallurgical Engineering, School of Chemical Engineering, Vuorimiehentie 2, 02150, Espoo, Finland

ARTICLE INFO

Keywords:

Copper recovery
Electrodeposition
Circular economy
Waste management

ABSTRACT

In this study, copper present in industrial waste water with a variety of other impurities (Fe, Mg, Al, Zn, As) was subjected for selective electrochemical recovery. The recovery was conducted directly on carbon nanostructures in order to create added-value products synergistically. In-depth electrochemical and structural analysis showed that single/multi-walled carbon nanotubes (CNTs) and graphene composites could provide an excellent substrate for Cu's electrochemical recovery. Furthermore, formulations based on them also enabled the formation of even Cu deposits on the surface directly from wastewater solutions without further bath condition adjustments. After just 1-h electrodeposition at -0.1V vs. SCE, a nanocomposite based on CNTs was obtained. Cu was recovered exclusively and accounted for 45% of the total weight of the composite.

1. Introduction

The hydrometallurgical industry plays a notable role in producing large quantities of metal-containing process and waste solutions. In particular, acidic industrial wastewaters may contain valuable metals, such as copper as well as less valuable elements such as iron, aluminum, magnesium. Cu solutions are toxic for plants (inhibit photosynthesis, plant growth, and reproductive process [1]) and aquatic organisms (cause deformities, diseases, or death [2]). The recommended safe content of Cu in water for aquatic life is as low as 2–4 ppb, whereas the acceptable upper level of Cu for humans is 10 mg/L. Consequently, any means to reduce the concentration of Cu or other elements in the environment are welcome since they are a growing concern [3–8]. Simultaneously, there is an evident increase in demand for copper in our everyday applications, increasing the need for hydrometallurgical copper operations substantially. Therefore, efficient removal and re-use of copper is attractive not only from an environmental but also from an economic point of view. Earlier, numerous treatment techniques have been applied to obtain valuable materials from waste water. Typically, however, metals are recovered not as a product but as waste residues.

Out of the various waste water treatment methods available, chemical precipitation is the most commonly utilized industry process due to its simplicity and low cost. However, precipitation by forming insoluble hydroxides or sulfides is not selective and requires the use of reagents, such as lime, calcium oxide, and hydrogen sulfide [9]. Following precipitation, the solids are then separated from the

* Corresponding author.

E-mail address: dawid.janas@gmail.com (D. Janas).

<https://doi.org/10.1016/j.wri.2021.100156>

Received 25 March 2021; Received in revised form 2 June 2021; Accepted 13 July 2021

Available online 24 July 2021

2212-3717/© 2021 The Author(s). Published by Elsevier B.V. This is an open access article under the CC BY-NC-ND license

(<http://creativecommons.org/licenses/by-nc-nd/4.0/>).

sludge by coagulation and/or sedimentation or filtration. The solids are then discarded as reprocessing into new raw material is not economical. Adsorption is another possible method for heavy metal removal, and a plethora of different adsorbents have been studied, including active carbon [10], geopolymers [11], and clay [12]. While these methods can remove heavy metals from solutions, the removal needs to be followed by further process steps before reuse of the metals is possible, if at all. On the other hand, electrodeposition is a method that can deposit metals selectively onto conducting materials even from solutions of low metal concentration [13]. High standard electrode potential ($E^0 = 0.34$ V vs. SHE) of copper provides a unique feature among typical waste water impurities for electrochemical recovery, as it can enable high selectivity even from multimetallic solutions. This can also allow direct recovery of Cu on nanomaterials, avoiding the use of high-quality synthetic chemicals and deposition baths typically used to make such nanocomposites. Direct and selective recovery leading to value-added products may also pave the way for new business models related to waste water treatment.

One of the most outstanding nanomaterials are those made of carbon [8,14–18]. They provide remarkably tunable thermal conductivity (0.028–6600 W/m·K) [19], leading strength (Young's modulus 270–950 GPa) [20], and adjustable surface chemistry [21, 22]. Nowadays, carbon nanotube (CNT) networks attain electrical conductivity up to 5000 S/cm for pristine and 20,000 S/cm for doped material [23]. To enhance nanocarbon's electrical properties, one can combine them with other conductive materials [24]. Cu-CNT composite revealed two orders of magnitude higher current carrying capacity [25] compared to Cu standard. Besides, the thermal and mechanical properties of Cu-CNT are often encouraging [26–29]. Thus, because of high thermal and electrical conductivity and the relatively good chemical stability of Cu, it is an attractive admixture for producing high-performance composites with CNTs or graphene [26]. There is a vast spectrum of possible applications for such materials, which spans from supercapacitors [30,31], biosensors [32] to electrical conductors [33]. The low-weight of composites combined with high strength and notable electrical conductivity make them particularly promising for application in overhead transmission lines [33] or automotive and aerospace industries [26].

There are many ways to produce Cu-CNT materials. Depending on the process character, they can be separated into powder processing, electrochemical deposition, and electroless deposition. In powder metallurgy methods, powders of nanocarbon and Cu are often mixed using ball/attrition milling [34–38], sonication [29,39,40], isostatic pressing [41,42], stirring [43], or vortex mixing [44], and then they are compacted. In this case, the process is straightforward and scalable, providing a large amount of composite [33,45]. An alternative is to coat one material with the other by e.g. electroplating [46], which is a well-known electrochemical method to make Cu-CNT materials [13,47–49].

In this work, we made a direct Cu recovery from waste water on thin free-standing films based on CNTs for the first time. Based on a detailed analysis of the electrochemical parameters and the microstructure of the obtained materials, the critical parameters to make the electrochemical recovery of Cu from waste water on CNTs quick and homogeneous were established. The proposed method's universal character makes it relevant for a broad spectrum of carbon materials [50] [–] [52] and other conductive substrates.

2. Experimental

2.1. Waste waters investigated

Waste waters investigated were synthetic Cu electrodeposition bath (40 g Cu - 0.63 mol/dm³ Cu and 100 g of H₂SO₄ per 1 L - 1.02 mol/dm³ H₂SO₄) as well as authentic industrial process wastewater. The feed compositions are presented in Table 1. The values were determined by the Inductively Coupled Plasma - Optical Emission Spectrometer (ICP-OES) method.

2.2. Nanocarbon materials for Cu recovery

Several types of nanocarbon materials were used for the study, some of which were produced in-house, and the remainder was procured from commercial sources (where indicated). Multi-walled CNTs (MWCNTs) were synthesized by catalytic Chemical Vapour Deposition (c-CVD) [53,54]. The protocol is given in the Supplementary Information (SI).

Commercial materials used for the study included high-purity single-walled CNTs ($d \approx 1.5$ nm; TuballTM, OCSiAl, Luxembourg), technical-grade multi-walled CNTs ($d \approx 10$ nm; NC7000TM, Nanocyl, Belgium), and graphene nanoplatelets (C-300, Sigma-Aldrich, USA). According to the manufacturer, the graphene material is a few nm thick. In the manuscript, these materials are referred to as SWCNTs, NC-MWCNTs, and G, respectively. The materials were used without any post-processing, except for SWCNTs. They were ground for 5 min due to our earlier observation that the process increases the electrical conductivity of the films formed from them by causing appropriate deagglomeration [55].

The influence of oxidation was studied using MWCNTs made in-house. The methodology is given in the SI. The product is referred to as O-MWCNTs.

Thin films made of nanocarbon materials were manufactured using a previously reported method [56]. The film preparation

Table 1
Composition of employed solutions containing Cu.

Solution	Mg [mg/L]	Al [mg/L]	Fe [mg/L]	Ni [ppm]	Cu [ppm]	Zn [ppm]	As [ppm]	Sb [ppm]	Pb [ppm]
Synthetic solution	–	–	–	–	40.0×10^6	–	–	–	–
Industrial process wastewater	6600	1400	12,500	13	428	100	52	–	4.5

routine is described in the SI. A photograph of a flexible free-standing nanocarbon film used in the study, which can be manipulated easily (Fig. S1).

2.3. Electrochemical recovery of Cu

For each electrochemical experiment, a free-standing nanocarbon film was cut into a rectangular shape of 10 mm width x 25 mm length. A three-electrode cell with electrodes facing each other was used for all the electrochemical experiments. The film sample was used as the working electrode, whereas a platinum sheet with an order of magnitude larger area served as the counter electrode. The distance between the nanocarbon film and the platinum electrode was 5 cm. The film sample was immersed ca. 1.5 cm into the solution, and the current density values were calculated after the experiment using the observed submerged geometrical area. A standard calomel electrode (SCE) placed next to the nanocarbon film surface was used as the reference electrode. The electrodes were connected to an IviumStat 24-bit CompactStat potentiostat (Ivium Technologies, Netherlands), as shown below (Fig. 1).

For cathodic polarization experiments, the potential of the cathode stabilized during 60 s, and the equilibrated open circuit potential of the films was set as $E = 0$ V vs. SCE. The potential (E) was then changed from 0 V to -1 V with a sweep rate of 20 mV/s. Galvanostatic deposition i.e. chronoamperometry was used to deposit Cu onto the nanocarbon films.

To observe differences in nanocarbon films' surface activity, a small amount of Cu was deposited as separate nuclei on the CNT films by a galvanostatic deposition pulse. The deposition was made at 0 V vs. SCE for 1 s. The tests were carried out on all the nanocarbon films with and without the binder.

To validate the application potential, longer plating experiments were also conducted. For the recovery of Cu from wastewater, we used the following parameters: deposition voltage of -0.1 V vs. SCE for 3600 s. For these experiments, 6 nanocarbon films were selected: SWCNTs, NC-MWCNTs, MWCNTs, 25% O-MWCNTs, 25% N-MWCNTs, and 25% Graphene. All electrochemical processes were conducted at room temperature.

2.4. Characterization

Scanning Electron Microscopy (SEM, JEOL JSM-7500FA) was used to analyze the microstructure of the studied nanocarbon films. The samples were investigated at 15 kV acceleration voltage at the magnification of $16,000 \times$ for powder samples and $2200 \times$ for nanocarbon-Cu composites. Raman spectroscopy (Renishaw, Germany) was used to determine the quality of the parent nanocarbon materials and thin films made from them. All the powders and film samples were measured by this method. The measurement parameters were as follows: laser wavelength 514 nm, power 5%, objective 20x, and exposure time of 10 s. The measurements were conducted at multiple sample areas at several accumulations to reach statistical significance and minimize background noise. The films' electrical conductivity was measured by the 4-probe method using a 2182A source meter (Keithley, USA) under 100 mA electric current. A custom-made setup measured water Contact Angles (WCA) with a CMOS camera (Thorlabs, USA). In each case, 10 μ L of water was positioned onto the film surface, and the contact angle value was recorded based on the image recorded with the camera equipped with a macro lens. Multiple droplets were deposited onto every type of film for WCA measurements. Analysis by Inductively Coupled Plasma Optical Emission Spectroscopy (ICP-OES) was made (PerkinElmer Optima 7100 DV, USA) to characterize the chemical composition of the Cu-containing solutions. Energy-Dispersive X-ray Spectroscopy (EDX, JEOL JED-2300 Analysis Station) was used to analyze the composition of the surface of nanocarbon-Cu materials at 15 kV acceleration voltage.

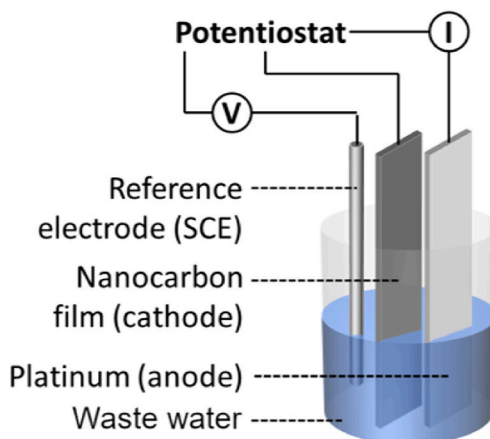


Fig. 1. Schematic of electrochemical Cu recovery by three-electrode setup.

3. Results and discussion

3.1. Characterization of nanocarbon substrates for Cu recovery

Characterization of the microstructure (Fig. S2) and purity of the parent carbon nanostructures (Fig. S3), provided in the SI, revealed that these materials have diverse morphology and degree of structural perfection. While the SWCNTs exhibited an extremely low amount of defects, the other materials showed a varying content of impurities and functional groups. These differences should make the materials more or less appropriate for Cu recovery. Thin films were made from such raw materials, and their properties were analyzed (before and after the removal of EC binder) to find the critical factors making such waste treatment process successful. Fig. 2 demonstrates the results of Raman spectroscopy, which gauges the level of crystallinity in nanocarbon materials.

For the neat CNT materials (SWCNTs, NC-MWCNTs, MWCNTs), I_D/I_G ratios (indicative of the perfectness of the material; the lower, the purer) decreased slightly after annealing. During this process, amorphous carbon, EC, and other forms of carbon were removed, which caused a decrease in intensity of defect-induced D peak. However, when O-doped MWCNT materials were briefly exposed to the influence of high temperature, the I_D/I_G ratios were considerably reduced. The effect was more pronounced at a high content of O-MWCNTs (50%, $I_D/I_G = 0.032 \pm 0.001 \rightarrow I_D/I_G = 0.017 \pm 0.001$) as compared with a low concentration of O-MWCNTs (10%, $I_D/I_G = 0.018 \pm 0.001 \rightarrow I_D/I_G = 0.010 \pm 0.001$) in the composite with SWCNTs. The decrease of I_D/I_G at high content of O-MWCNTs could be explained by the detachment of the most severely oxidized species during annealing, which would overall improve the average degree of structural perfection of the material after annealing [57]. Regarding the N-doped samples, the I_D/I_G ratios remained at a comparable level before and after annealing (10%, $I_D/I_G = 0.017 \pm 0.003 \rightarrow I_D/I_G = 0.013 \pm 0.003$; 25%, $I_D/I_G = 0.014 \pm 0.002 \rightarrow I_D/I_G = 0.013 \pm 0.003$; 50%, $I_D/I_G = 0.015 \pm 0.001 \rightarrow I_D/I_G = 0.013 \pm 0.001$). Lastly, in the case of doping of SWCNTs with graphene, taking into account the uncertainty values, the I_D/I_G ratios were not affected by the thermal processing.

Analysis of the whole dataset revealed that every time high-quality SWCNTs were used to form composites with other nanocarbon types, the signals from SWCNTs dominated the spectra. Despite that SWCNTs are combined with materials of relatively high I_D/I_G ratios (e.g., 0.434, 0.518, and 0.620 for O-MWCNTs, N-MWCNTs, and graphene, respectively), the resulting I_D/I_G ratio was low. It did not exceed 0.02 in virtually all cases, even when up to 1:1 w/w of functionalized nanocarbon was added to the SWCNT matrix. Resonant Raman scattering excites only a subset of the CNT population, which may lead to a bias in interpreting results [58]. In this study, it appears that the intensity of signal coming from SWCNTs dominated that of the MWCNTs because more of the SWCNTs were in tune with the selected laser wavelength.

One of the critical parameters for the successful Cu recovery is the substrate's appropriate surface chemistry, which ensures compatibility with the aqueous plating solution. The lower the value of the water contact angle (γ), the higher the likelihood that the nanocarbon film, which is often inherently hydrophobic, will be successfully plated with Cu [59,60]. Hence we decided to study this factor (Fig. 3). The films from parent nanocarbon materials containing the binder had a relatively hydrophobic surface ($\gamma > 90^\circ$). However, after its removal by annealing, we observed a radical decrease in WCA for these samples (SWCNTs: $\gamma_{\text{with binder}} = 113.6 \pm 5.6^\circ \rightarrow \gamma_{\text{without binder}} = 39.3 \pm 6.6^\circ$ - Fig. S4, NC-MWCNTs: $\gamma_{\text{with binder}} = 111.6 \pm 4.8^\circ \rightarrow \gamma_{\text{without binder}} = 7.9 \pm 1.7^\circ$, and MWCNTs: $\gamma_{\text{with binder}} = 95.42 \pm 8.2^\circ \rightarrow \gamma_{\text{without binder}} = 9.0 \pm 2.4^\circ$). This phenomenon was observed in our previous works. It was possibly caused by the thermal desorption of impurities from the ambient, which apparently cloaked the CNT surface's hydrophilic nature [53,61].

Furthermore, the composite materials based on the SWCNT matrix (containing N-MWCNTs, O-MWCNTs, and graphene) had less hydrophobic character (ca. $\gamma = 70\text{--}80^\circ$). These filler materials are characterized by a relatively high level of disorder, which made them more hydrophilic. After annealing, all these materials reached the WCA of up to ca. 20° . The recorded values were roughly halfway between that of the SWCNT matrix and the MWCNTs fillers, from which these composite materials were formed. The elevated

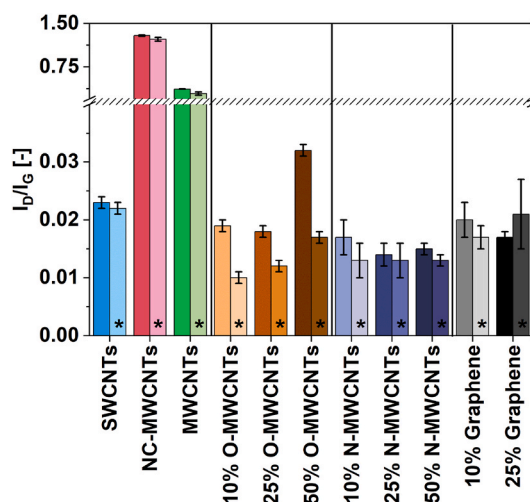


Fig. 2. I_D/I_G ratios for nanocarbon films before and after removal of the EC binder (indicated with an asterisk).

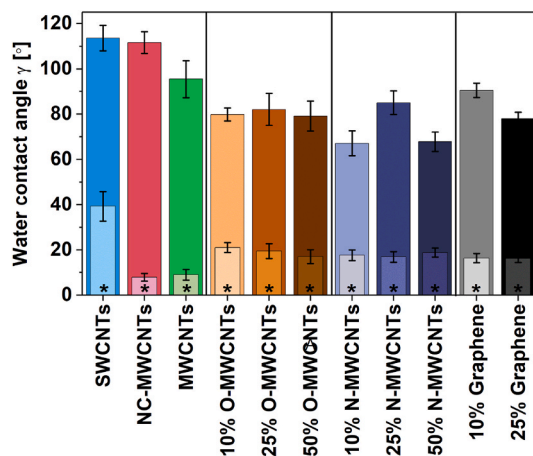


Fig. 3. Water contact angles for nanocarbon films before and after removal of EC binder by annealing (overlaid, indicated with an asterisk).

value of WCA for SWCNTs was likely related to the fact that the films made from them had a different roughness than those produced from NC-MWCNTs or MWCNTs [62,63].

Nanocarbon films' electrical conductivity directly affects their electrochemical activity, which is one of the prerequisites for successful Cu recovery, and thus it requires investigation (Fig. 4). Our previously published results [54,55,64] indicate that the material pre-processing and presence of binder/doping agents are significant factors to consider. In this work, the highest electrical conductivity was recorded for high-quality SWCNT films (1064.0 ± 69.0 S/cm). Conversely, the electrical conductivity of MWCNT samples composed of technical grade (NC-MWCNTs) or in-house-made (MWCNTs) was low: 36.8 ± 0.5 S/cm and 123.9 ± 18.3 S/cm, respectively. This was due to the abundance of defects and inherently worse electrical conductivity of MWCNTs than SWCNTs [65].

When SWCNTs were used to form composite materials with O-MWCNTs, N-MWCNTs, or graphene, these hybrids had, on average 6 times lower electrical conductivity (by 5.4, 7.4, and 6.2 times, respectively) than neat SWCNTs. Deterioration of electrical conductivity can be explained by a significant content of defects in the admixed nanocarbon types as detected by Raman spectroscopy. Due to the increased abundance of imperfections, charge scattering is more pronounced, which elevates the resistance. Unfortunately, the electrical conductivity of films made exclusively from O-MWCNTs, N-MWCNTs, or graphene could not be determined because the films produced from them had poor mechanical integrity.

Furthermore, we examined the impact of binder removal on the electrical conductivity of the nanocarbon ensembles. The annealing of the material did not seem to affect the electrical conductivity of SWCNTs, NC-MWCNTs, or MWCNTs, which stayed in accordance with Raman's characterization showing no change to the structure of the material during thermal treatment [55,64]. However, after annealing, the value of electrical conductivity for all the composites of SWCNTs with O-MWCNTs, N-MWCNTs and graphene almost doubled (e.g. 50% O-MWCNTs: $\sigma_{\text{with binder}} = 82.7 \pm 15.3$ S/cm \rightarrow $\sigma_{\text{without binder}} = 166.8 \pm 23.3$ S/cm or 25% N-MWCNTs: $\sigma_{\text{with binder}} = 99.3 \pm 3.3$ S/cm \rightarrow $\sigma_{\text{without binder}} = 148.7 \pm 8.5$ S/cm). We believe that the surface chemistry of CNTs became much more compatible with the EC structure after implanting O- and N-functionalities into these nanocarbon materials. Likely, oxygen-rich EC binder

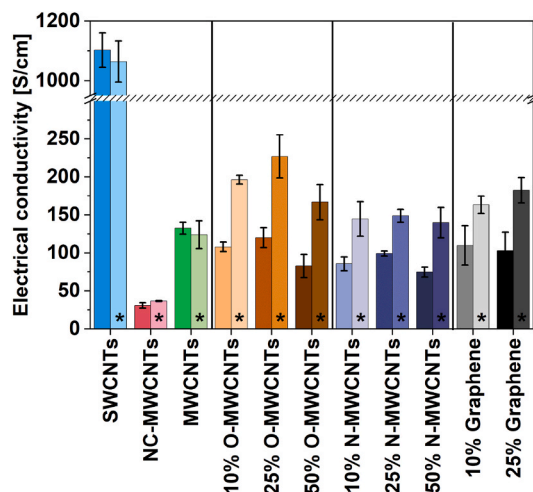


Fig. 4. Electrical conductivity values of nanocarbon films before and after removal of the EC binder (indicated with an asterisk).

interacted very well with modified CNTs (O-MWCNTs and N-MWCNTs). This, in turn, led to the encapsulation of O-MWCNTs and N-MWCNTs by a dielectric EC binder, which impeded the electrical conductivity of the material. Therefore, when the EC was removed by annealing, the electrical conductivity increased due to the formation of new percolation pathways. The same mechanism can explain the increase of electrical conductivity SWCNTs/graphene composites upon annealing due to the abundance of graphene base material defects as determined by Raman spectroscopy.

To sum up, the electrical conductivities of all binder-free nanocarbon composites of SWCNTs with functionalized MWCNTs or graphene showed similar values of about 150–200 S/cm. What regards the base materials after annealing, the notable exceptions were the highly conductive SWCNT films (conductivity of 1064.0 ± 69.0 S/cm) and poorly conductive NC-MWCNTs (conductivity of 36.8 ± 0.5 S/cm), which was mainly caused by the remarkably high and low quality of the material, respectively, as mentioned in text before.

3.2. Electrochemical recovery of Cu onto nanocarbon films

3.2.1. Cathodic polarization experiments

Cathodic polarization curves were recorded for all samples in synthetic Cu waste water (Fig. 5). The results showed typical characteristics of Cu recovery by electrodeposition from a high concentration solution with some notable differences in deposition kinetics between various samples. Two distinctive sets of behaviors were observed in all curves: (i) slow recovery kinetics for all samples containing binder and samples consisting purely of unfunctionalized MWCNTs and (ii) fast recovery kinetics for all binder-free samples, including neat SWCNTs and their composites with functionalized MWCNTs.

The samples showing slow deposition kinetics (i) demonstrated a slow change in Cu deposition current with the function of overvoltage. These samples showed a cathodic deposition slope ranging from 0.06 to 0.16 mA/mV. The films produced from commercial MWCNTs (NC-MWCNT) exhibited the slowest deposition kinetics with or without binder, which was attributed to the significantly lower electrical conductivity compared with other samples. The binder presence clearly decreased Cu's recovery rate due to its insulating properties leading to physical blocking of the underlying nanocarbon network. Furthermore, as the binder containing samples were more hydrophobic, it was deduced that the binder's presence made the penetration of the electrolyte into the film more difficult, thus leading to less surface area exposed for deposition as shown previously [66].

Conversely, the high polarization samples (ii) showed a considerably steeper cathodic slope, which meant that the material polarized more easily for the deposition of Cu. The cathodic deposition slope was in the range of 0.18–0.45 mA/mV. The observed faster kinetics could not be ascribed to increases in electrical conductivity but only to the removal of binder. Lastly, no obvious correlation between the cathodic deposition slope (Table 3) and electrical conductivity could be made (Fig. 4).

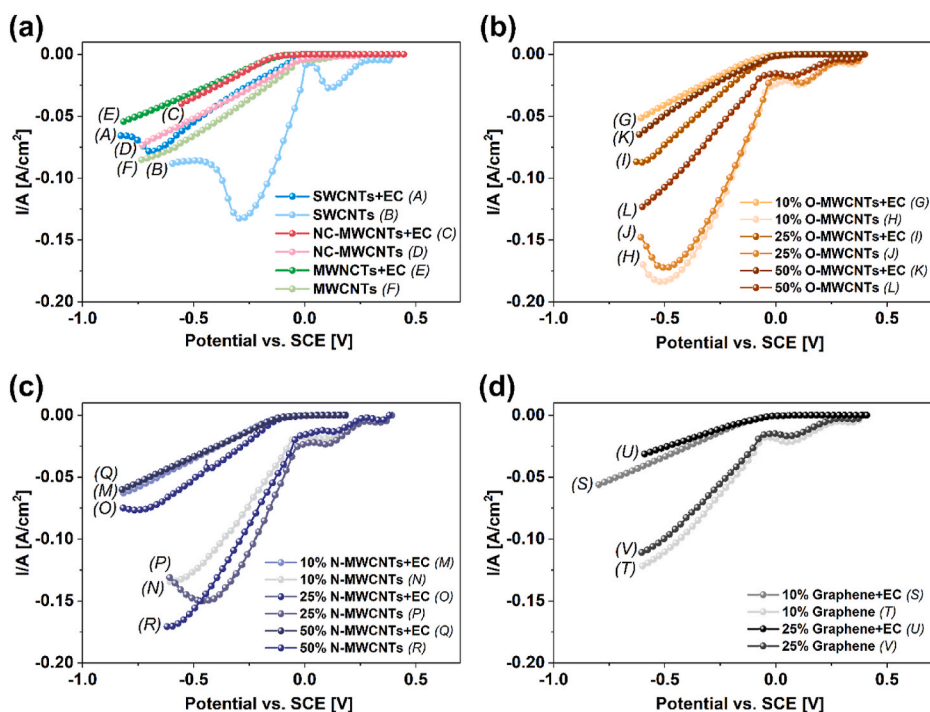


Fig. 5. Cathodic polarization curves for (a) neat CNT films, (b) oxygen-doped CNT films, (c) nitrogen-doped CNT films, and (d) graphene-doped CNT films.

3.2.2. Pulsed electrochemical recovery of Cu

To further test the performance of various nanocarbon film materials, the pulsed recovery i.e. pulse electrodeposition of Cu particles was studied from the synthetic electrolyte. For this experiment, the samples were electrodeposited with a single deposition pulse of 1 s at 0.0 V vs. SCE. The purpose of using such low overvoltage for Cu deposition was to examine the differences between samples with different compositions and functionalities and the effect of the binder on the very first nuclei forming in the beginning stages of Cu deposition.

We first examined the parent materials (Fig. 6a). The results showed that the pulse electrodeposition process was most facile on neat SWCNTs. Round Cu clusters of about 2 μm in diameter were distributed evenly near the surface of the film. It was noted that when the SWCNTs contained the binder (Fig. 6b), the Cu deposition was also pronounced, but the size, shape, and distribution of the particles were less uniform. Therefore, the removal of the binder was found to be beneficial for the deposition of homogeneously distributed Cu nuclei, confirming the results from the cathodic polarization experiments.

On the other hand, when MWCNTs were employed, only scarce Cu clusters could be observed on the surface (Fig. 6c and d). The reason why Cu's electrodeposition was inferior on these types of films could be ascribed to the low values of electrical conductivity and poor crystallinity (high I_D/I_G ratio, as shown in Fig. 2). NC-MWCNTs and MWCNTs had an order of magnitude lower electrical conductivity than SWCNTs and were characterized by an abundance of defects. Consequently, the electrodes made from them were more challenging to polarize, as shown in Fig. 5, leading to reduced Cu deposition kinetics. Hence, only a negligible amount of Cu on the surface was observed after the deposition. Moreover, since Cu deposition is favored on the defects, which are abundant in these materials, Cu's inhomogeneous distribution was noted.

In the next step, we wanted to find out how the incorporation of functionalized MWCNTs into the SWCNT matrix would affect the ability of the material to be deposited with Cu (Fig. 7). Previously, it has been shown that incorporating oxygen-containing functionalities on the surface of CNT films improved the electrochemical response for metal electrodeposition due to higher reactivity of oxygen-containing functional groups [66], giving rise to a more homogeneous distribution of smaller metal nuclei.

In this work, the same general trend was observed to a certain degree. Increasing the amount of functionalized MWCNTs while reducing the amount of SWCNTs led to smaller Cu nuclei up to 25% O-MWCNTs. At 10%–25% of O-MWCNTs (Fig. 7a and b), only smaller Cu deposits at a maximum of a few microns in diameter were detected, which were distributed evenly across the sample surface. However, higher amounts of O-MWCNTs (Fig. 7c) resulted in sparsely situated ca. 10 μm Cu nuclei, similar to the pure MWCNT material. The results were in line with the polarization experiments, which showed that the slope of the deposition was similar for samples consisting of only SWCNTs and for samples containing 10% and 25% O-MWCNTs. Conversely, at 50% O-MWCNTs, the cathodic slope showed a clear decrease, which was likely related to the high amount of less conductive MWCNTs that negatively affected the polarization's ability. Therefore, only small additions of functionalized CNTs were beneficial for the deposition of evenly distributed small Cu nuclei compared with pure SWCNT material. These results prove that instead of oxidation of the bulk SWCNT material, a more facile strategy can be employed. A certain amount of oxidized CNTs can be simply admixed to the SWCNT matrix to promote the process.

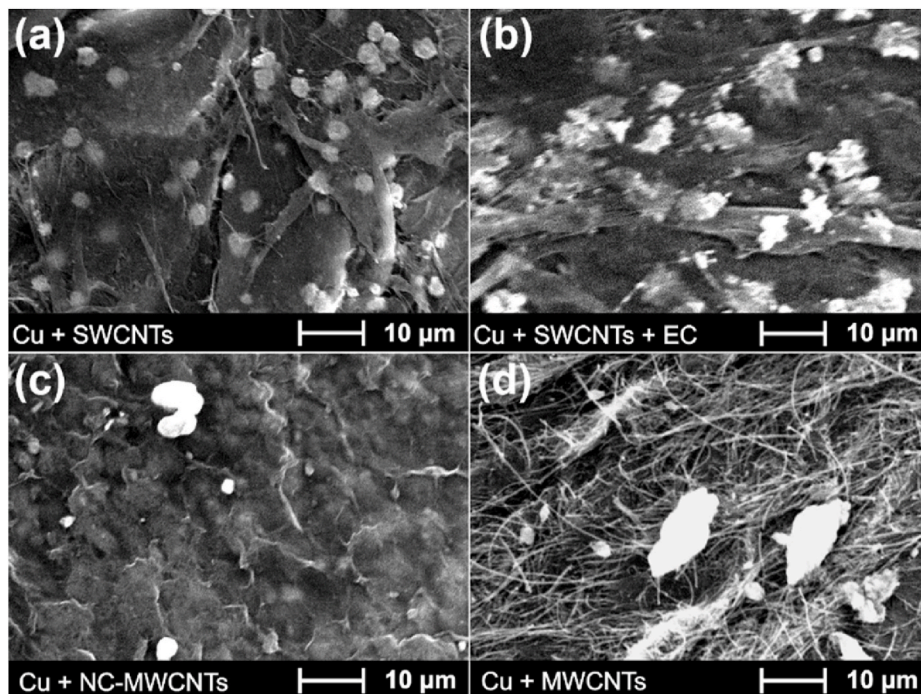


Fig. 6. SEM micrographs of Cu deposited on films from parent CNTs after pulse electrodeposition.

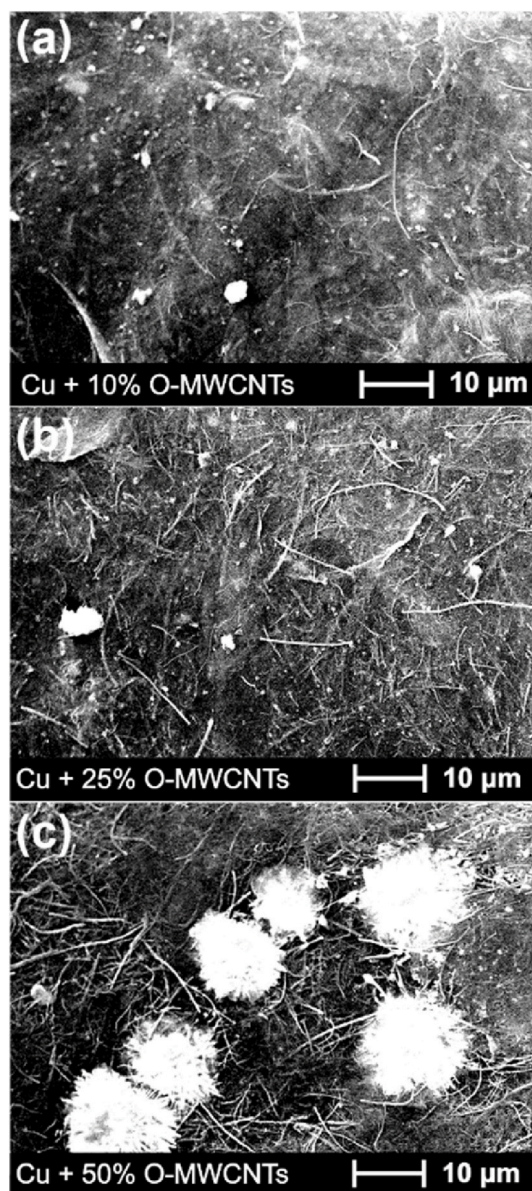


Fig. 7. SEM micrographs of Cu deposited on films from SWCNTs and O-MWCNTs after pulse electrodeposition.

Considering the composite films made of N-MWCNT and graphene fillers, their addition on the level of 25% in the SWCNT matrix did not promote homogeneous Cu deposition (Fig. 8). For both types of these composite films, the deposition was sparse, and the size and distribution of the particles varied considerably. No pattern of Cu nuclei size could be discerned.

3.2.3. Cu recovery from industrial waste water

Authentic industrial waste water was employed to test the nanocarbon composite films' applicability for the direct Cu recovery from wastewater. Different types of films were selected for 1-h electrodeposition at -0.1V vs. SCE. Such electrodeposition potential was chosen as it was not low enough to deposit the less noble elements from the solution. These conditions allowed only Cu (and more noble elements) to be reduced selectively on the film surface. The concentration of Cu (428 ppm) in wastewater was 100x lower than that of the synthetic Cu electrolyte. It contained a plethora of other metals, such as Fe, Al, and Mg in sulfate-rich media (Table 2).

SEM micrographs in Fig. 9 show the morphology of the Cu particles deposited on various types of nanocarbon films from this feed. The sizes of Cu deposits on films were SWCNTs ($1.5 \pm 0.3 \mu\text{m}$), MWCNTs ($4.3 \pm 0.5 \mu\text{m}$), and 25% graphene ($1.1 \pm 0.3 \mu\text{m}$). For the remaining materials, the size distribution was too inhomogeneous to determine this value with any certainty. Generally, the Cu deposits' size followed the same trend, as noted previously, with the MWCNT film showing larger particles. No deposits could be discerned on the NC-MWCNT film, likely due to its low conductivity not being able to support deposition at such overvoltage. However,

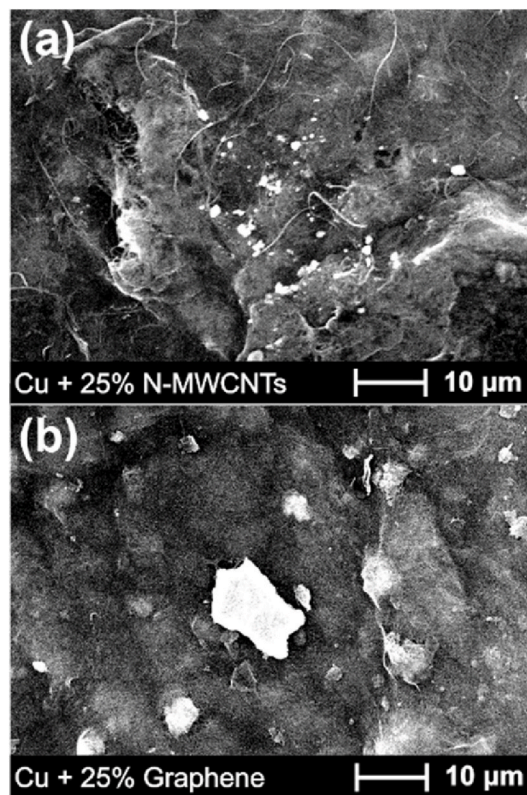


Fig. 8. SEM micrographs of Cu deposited on films from SWCNTs and N-MWCNTs or graphene after pulse electrodeposition.

Table 2

List of nanocarbon films used in the study.

Short Name	Composition
SWCNTs	Commercial high-quality single-walled CNTs
NC-MWCNTs	Commercial technical grade multi-walled CNTs
MWCNTs	In-house made multi-walled CNTs
10% O-MWCNTs	Oxidized in-house made multi-walled CNTs & single-walled CNTs (1:9, w/w)
25% O-MWCNTs	Oxidized in-house made multi-walled CNTs & single-walled CNTs (1:3, w/w)
50% O-MWCNTs	Oxidized in-house made multi-walled CNTs & single-walled CNTs (1:1, w/w)
10% N-MWCNTs	N-doped in-house made multi-walled CNTs & single-walled CNTs (1:9, w/w)
25% N-MWCNTs	N-doped in-house made multi-walled CNTs & single-walled CNTs (1:3, w/w)
50% N-MWCNTs	N-doped in-house made multi-walled CNTs & single-walled CNTs (1:1, w/w)
10% Graphene	Graphene & single-walled CNTs (1:9, w/w)
25% Graphene	Graphene & single-walled CNTs (1:3, w/w)

Note: 50% Graphene composite was not used in the study because it revealed poor mechanical properties after preparation.

the even size and distribution of the Cu deposits on SWCNT films appeared encouraging; therefore, we subjected it to further analysis.

EDX mapping and spectral analysis of the deposited particles (Fig. 10) confirmed that they were pure Cu (>45 wt%), and no other metallic elements were present. Oxygen (≈ 10 wt%) was also detected in the areas corresponding to Cu, which indicated that these species are either partially oxidized, or there were some deposits on the surface containing oxygen. Nevertheless, the lack of other elements besides carbon in the spectrum proved that not only the Cu deposition was successful from a complex mixture of elements, but that the process also exhibited selectivity after application of appropriate conditions. Taken together, these results illustrate that the proposed integration strategy of Cu and nanocarbon is selective and can be used to manufacture high-quality composites directly from waste solutions.

4. Conclusions

This work examined the recovery of copper directly on various types of films made from nanocarbon materials used as admixed

Table 3
Summary of cathodic deposition results.

Sample	Cathodic deposition slope [mA/mV]
SWCNTs + EC	0.12
SWCNTs	0.45
MWCNTs + EC	0.08
MWCNTs	0.12
NC-MWCNTs + EC	0.09
NC-MWCNTs	0.10
10% O-MWCNTs + EC	0.09
10% O-MWCNTs	0.40
25% O-MWCNTs + EC	0.16
25% O-MWCNTs	0.36
50% O-MWCNTs + EC	0.11
50% O-MWCNTs	0.20
10% N-MWCNTs + EC	0.09
10% N-MWCNTs	0.24
25% N-MWCNTs + EC	0.13
25% N-MWCNTs	0.35
50% N-MWCNTs + EC	0.08
50% N-MWCNTs	0.30
10% Graphene + EC	0.08
10% Graphene	0.20
25% Graphene + EC	0.06
25% Graphene	0.18

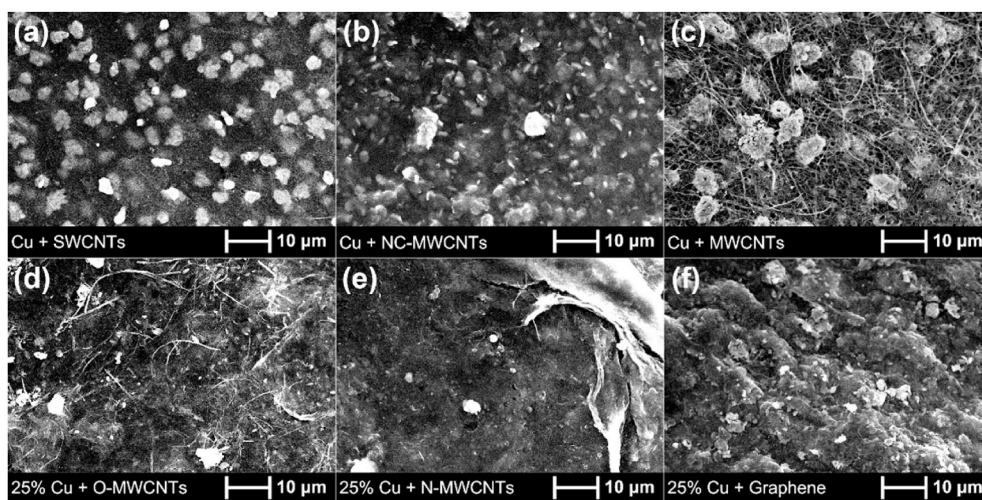


Fig. 9. SEM micrographs of Cu deposits on various nanocarbon films after 1h of electrodeposition from wastewater.

material for electrochemical recovery of Cu. The materials were extensively characterized to understand the electrodeposition process. Firstly, recovery from synthetic Cu electrolyte (40 g/L Cu) was studied using cathodic polarization experiments and pulse electrodeposition to observe differences in electrochemical and Cu nucleation behavior. Furthermore, an authentic industrial multi-metallic wastewater solution containing 428 ppm Cu was utilized as the raw material. The obtained results showed a beneficial response when using films with higher electrical conductivity and films containing different functional groups to cover the surface with Cu evenly.

The results validate that direct recovery of copper from industrial waste water on nanocarbon substrates is possible, as nano-materials' microstructure can be tuned with ease and to a large extent. Due to the rich chemistry of carbon, it is straightforward to optimize the topography and chemical composition to make nanocarbon integrate well with Cu. Consequently, added value composite materials can be produced even when industrial waste water solution is taken as the source of metal nanoparticles. This way, the problematic waste is not only managed but transformed into products of high added value. It is envisioned that the structures produced by this approach can show particular promise for catalytic or electrochemical applications. In these scenarios, the combination of a highly conductive substrate with the unique properties of size constrained metal nanoparticles paves the way towards reaching high performance on these fronts.

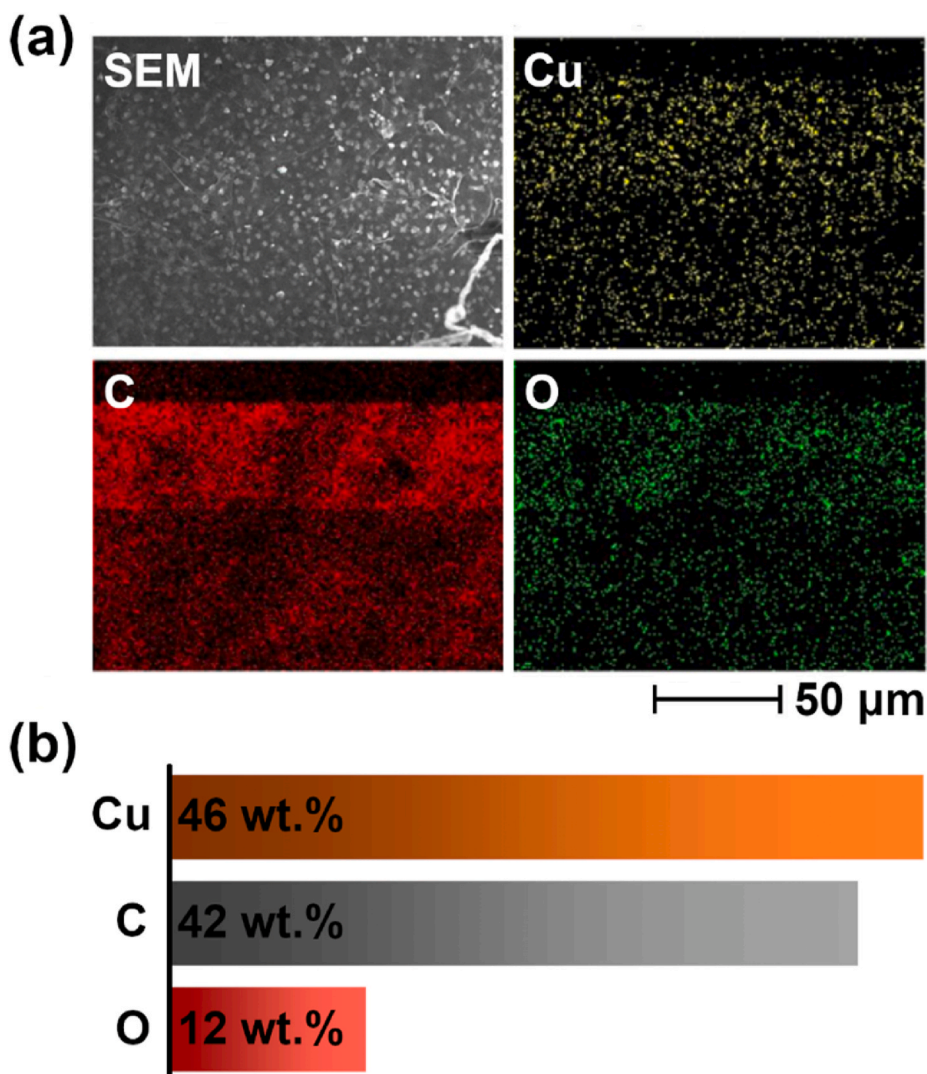


Fig. 10. (a) EDX mapping of a Cu-SWCNT composite and the (b) quantitative analysis.

Declaration of competing interest

The authors declare that they have no known competing financial interests or personal relationships that could have appeared to influence the work reported in this paper.

Acknowledgments

G.S, B.K, and D.J. would like to thank the National Center for Research and Development, Poland (under the Leader program, grant agreement LIDER/0001/L-8/16/NCBR/2017). G.S. and D.J. also acknowledge the National Agency for Academic Exchange of Poland (under the Academic International Partnerships program, grant agreement PPI/APM/2018/1/00004) for supporting training in the Aalto University, which enabled the execution of the study. G.S. acknowledges the Ministry of Science and Higher Education of Poland for financial support of scientific work from budget funds for science in the years 2019–2023 as a research project under the “Diamond Grant” program (grant agreement 0036/DIA/201948). P-M.H. and M.L. acknowledge the support of the “NoWASTE” project (Grant 297962) funded by Academy of Finland.

Appendix A. Supplementary data

Supplementary data to this article can be found online at <https://doi.org/10.1016/j.wri.2021.100156>.

Author statement

Grzegorz Stando: Conceptualization, Investigation, Data curation, Visualization, Writing - Original Draft. Pyry-Mikko Hannula: Methodology, Supervision. Bogumiła Kumanek: Validation. Mari Lundström: Resources, Funding acquisition, Supervision, Writing - Review & Editing. Dawid Janas: Conceptualization, Resources, Funding acquisition, Data curation, Visualization, Supervision, Project administration, Writing - Review & Editing.

References

- [1] R. Singh, N. Gautam, A. Mishra, R. Gupta, Heavy metals and living systems: an overview, *Indian J. Pharmacol.* 43 (2011) 246–253, <https://doi.org/10.4103/0253-7613.81505>.
- [2] G.S. Simate, S. Ndlovu, Acid mine drainage: challenges and opportunities, *J. Environ. Chem. Eng.* 2 (2014) 1785–1803, <https://doi.org/10.1016/j.jece.2014.07.021>.
- [3] A.A. Basheer, Chemical chiral pollution: impact on the society and science and need of the regulations in the 21st century, *Chirality* 30 (2018) 402–406, <https://doi.org/10.1002/chir.22808>.
- [4] A.A. Basheer, I. Ali, Stereoselective uptake and degradation of (\pm)-o,p-DDD pesticide stereoisomers in water-sediment system, *Chirality* 30 (2018) 1088–1095, <https://doi.org/10.1002/chir.22989>.
- [5] A.A. Basheer, New generation nano-adsorbents for the removal of emerging contaminants in water, *J. Mol. Liq.* 261 (2018) 583–593, <https://doi.org/10.1016/j.molliq.2018.04.021>.
- [6] I. Ali, C.K. Jain, Groundwater contamination and health hazards by some of the most commonly used pesticides, *Curr. Sci.* 75 (1998) 1011–1014. <http://www.jstor.org/stable/24101777>.
- [7] I. Ali, V.K. Gupta, H.Y. Aboul-Enein, Metal ion speciation and capillary electrophoresis: application in the new millennium, *Electrophoresis* 26 (2005) 3988–4002, <https://doi.org/10.1002/elps.200500216>.
- [8] I. Ali, O.M.L. Alharbi, Z.A. AlOthman, A.M. Al-Mohaimed, A. Alwarthan, Modeling of fenuron pesticide adsorption on CNTs for mechanistic insight and removal in water, *Environ. Res.* 170 (2019) 389–397, <https://doi.org/10.1016/j.envres.2018.12.066>.
- [9] F. Fu, Q. Wang, Removal of heavy metal ions from wastewaters: a review, *J. Environ. Manag.* 92 (2011) 407–418, <https://doi.org/10.1016/j.jenvman.2010.11.011>.
- [10] V. Strelko, D.J. Malik, M. Streat, Interpretation of transition metal sorption behavior by oxidized active carbons and other adsorbents, *Separ. Sci. Technol.* 39 (2005) 1885–1905, <https://doi.org/10.1081/SS-120030791>.
- [11] M.K. Khalid, V. Agarwal, B.P. Wilson, E. Takaluoma, M. Lundström, Applicability of solid process residues as sorbents for the treatment of industrial wastewaters, *J. Clean. Prod.* 246 (2020) 118951, <https://doi.org/10.1016/j.jclepro.2019.118951>.
- [12] S. Gu, X. Kang, L. Wang, E. Lichtfouse, C. Wang, Clay mineral adsorbents for heavy metal removal from wastewater: a review, *Environ. Chem. Lett.* 17 (2019) 629–654, <https://doi.org/10.1007/s10311-018-0813-9>.
- [13] P.M. Hannula, M.K. Khalid, D. Janas, K. Yliniemi, M. Lundström, Energy efficient copper electrowinning and direct deposition on carbon nanotube film from industrial wastewaters, *J. Clean. Prod.* 207 (2019) 1033–1039, <https://doi.org/10.1016/j.jclepro.2018.10.097>.
- [14] I. Ali, The quest for active carbon adsorbent substitutes: inexpensive adsorbents for toxic metal ions removal from wastewater, *Separ. Purif. Rev.* 39 (2010) 95–171, <https://doi.org/10.1080/15422119.2010.527802>.
- [15] N.H. Al-Shaalan, I. Ali, Z.A. AlOthman, L.H. Al-Wahaibi, H. Alabdulmonem, High performance removal and simulation studies of diuron pesticide in water on MWCNTs, *J. Mol. Liq.* 289 (2019) 111039, <https://doi.org/10.1016/j.molliq.2019.111039>.
- [16] I. Ali, Microwave assisted economic synthesis of multi walled carbon nanotubes for arsenic species removal in water: batch and column operations, *J. Mol. Liq.* 271 (2018) 677–685, <https://doi.org/10.1016/j.molliq.2018.09.021>.
- [17] I. Ali, A.A. Basheer, A. Kucherova, N. Memetov, T. Pasko, K. Ovchinnikov, V. Pershin, D. Kuznetsov, E. Galunin, V. Grachev, A. Tkachev, Advances in carbon nanomaterials as lubricants modifiers, *J. Mol. Liq.* 279 (2019) 251–266, <https://doi.org/10.1016/j.molliq.2019.01.113>.
- [18] A. Muhulet, F. Miculescu, S.I. Voicu, F. Schütt, V.K. Thakur, Y.K. Mishra, Fundamentals and scopes of doped carbon nanotubes towards energy and biosensing applications, *Mater. Today Energy.* 9 (2018) 154–186, <https://doi.org/10.1016/j.mtener.2018.05.002>.
- [19] B. Kumanek, D. Janas, Thermal conductivity of carbon nanotube networks: a review, *J. Mater. Sci.* 54 (2019) 7397–7427, <https://doi.org/10.1007/s10853-019-03368-0>.
- [20] M.F. Yu, O. Lourie, M.J. Dyer, K. Moloni, T.F. Kelly, R.S. Ruoff, Strength and breaking mechanism of multiwalled carbon nanotubes under tensile load, *Science* 84 287 (2000) 637–640, <https://doi.org/10.1126/science.287.5453.637>.
- [21] K. Balasubramanian, M. Burghard, Chemically functionalized carbon nanotubes, *Small* 1 (2005) 180–192, <https://doi.org/10.1002/sml.200400118>.
- [22] X. Wang, G. Shi, An introduction to the chemistry of graphene, *Phys. Chem. Phys.* 17 (2015) 28484–28504, <https://doi.org/10.1039/c5cp05212b>.
- [23] A. Lekawa-Raus, T. Gizewski, J. Patmore, L. Kurzepa, K.K. Koziol, Electrical transport in carbon nanotube fibres, *Scripta Mater.* 131 (2017) 112–118, <https://doi.org/10.1016/j.scriptamat.2016.11.027>.
- [24] C. Tang, H.-F. Wang, X. Chen, B.-Q. Li, T.-Z. Hou, B. Zhang, Q. Zhang, M.-M. Titirici, F. Wei, Topological defects in metal-free nanocarbon for oxygen electrocatalysis, *Adv. Mater.* 28 (2016) 6845–6851, <https://doi.org/10.1002/adma.201601406>.
- [25] C. Subramaniam, T. Yamada, K. Kobashi, A. Sekiguchi, D.N. Futaba, M. Yumura, K. Hata, One hundred fold increase in current carrying capacity in a carbon nanotube-copper composite, *Nat. Commun.* 4 (2013), <https://doi.org/10.1038/ncomms3202>.
- [26] D. Janas, B. Liszka, Copper matrix nanocomposites based on carbon nanotubes or graphene, *Mater. Chem. Front.* 2 (2018) 22–35, <https://doi.org/10.1039/c7qm00316a>.
- [27] R.K. Khisamov, K.S. Nazarov, L.R. Zubairov, A.A. Nazarov, R.R. Mulyukov, I.M. Safarov, S.N. Sergeev, I.I. Musabirov, D.D. Phuong, P.V. Trinh, N.V. Luan, P. N. Minh, N.Q. Huan, Fabrication, microstructure, and microhardness of copper composites reinforced by carbon nanotubes, *Phys. Solid State* 57 (2015) 1206–1212, <https://doi.org/10.1134/S1063783415060177>.
- [28] C. Arnaud, F. Lecouturier, D. Mesguich, N. Ferreira, G. Chevallier, C. Estournès, A. Weibel, C. Laurent, High strength - high conductivity double-walled carbon nanotube - copper composite wires, *Carbon N. Y.* 96 (2016) 212–215, <https://doi.org/10.1016/j.carbon.2015.09.061>.
- [29] R. Jiang, X. Zhou, Q. Fang, Z. Liu, Copper-graphene bulk composites with homogeneous graphene dispersion and enhanced mechanical properties, *Mater. Sci. Eng.* 654 (2016) 124–130, <https://doi.org/10.1016/j.msea.2015.12.039>.
- [30] M. Ciszewski, D. Janas, K.K. Koziol, Copper-decorated CNTs as a possible electrode material in supercapacitors, *Batteries* 5 (2019) 60, <https://doi.org/10.3390/batteries5030060>.
- [31] W.A.D.M. Jayathilaka, A. Chinnappan, S. Ramakrishna, A review of properties influencing the conductivity of CNT/Cu composites and their applications in wearable/flexible electronics, *J. Mater. Chem. C.* 5 (2017) 9209–9237, <https://doi.org/10.1039/C7TC02965A>.
- [32] B. Bajaj, H.I. Joh, S.M. Jo, G. Kaur, A. Sharma, M. Tomar, V. Gupta, S. Lee, Controllable one step copper coating on carbon nanofibers for flexible cholesterol biosensor substrates, *J. Mater. Chem. B.* 4 (2016) 229–236, <https://doi.org/10.1039/C5TB01781E>.
- [33] R.M. Sundaram, A. Sekiguchi, M. Sekiya, T. Yamada, K. Hata, Copper/carbon nanotube composites: research trends and outlook, *R. Soc. Open Sci.* 5 (2018) 180814, <https://doi.org/10.1098/rsos.180814>.

- [34] S.J. Yoo, S.H. Han, W.J. Kim, A combination of ball milling and high-ratio differential speed rolling for synthesizing carbon nanotube/copper composites, *Carbon* N. Y. 61 (2013) 487–500, <https://doi.org/10.1016/j.carbon.2013.04.105>.
- [35] Z. Huang, Z. Zheng, S. Zhao, S. Dong, P. Luo, L. Chen, Copper matrix composites reinforced by aligned carbon nanotubes: mechanical and tribological properties, *Mater. Des.* 133 (2017) 570–578, <https://doi.org/10.1016/j.matdes.2016.08.021>.
- [36] W. Li, D. Li, Q. Fu, C. Pan, Conductive enhancement of copper/graphene composites based on high-quality graphene, *RSC Adv.* 5 (2015) 80428–80433, <https://doi.org/10.1039/c5ra15189a>.
- [37] S. Zhao, Z. Zheng, Z. Huang, S. Dong, P. Luo, Z. Zhang, Y. Wang, Cu matrix composites reinforced with aligned carbon nanotubes: mechanical, electrical and thermal properties, *Mater. Sci. Eng.* 675 (2016) 82–91, <https://doi.org/10.1016/j.msea.2016.08.044>.
- [38] N. Nayan, A.K. Shukla, P. Chandran, S.R. Bakshi, S.V.S.N. Murty, B. Pant, P.V. Venkitakrishnan, Processing and characterization of spark plasma sintered copper/carbon nanotube composites, *Mater. Sci. Eng.* 682 (2017) 229–237, <https://doi.org/10.1016/j.msea.2016.10.114>.
- [39] C. Arnaud, F. Lecouturier, D. Mesguich, N. Ferreira, G. Chevallier, C. Estournès, A. Weibel, C. Laurent, High strength - high conductivity double-walled carbon nanotube - copper composite wires, *Carbon* N. Y. 96 (2016) 212–215, <https://doi.org/10.1016/j.carbon.2015.09.061>.
- [40] C. Guiderdoni, E. Pavlenko, V. Turq, A. Weibel, P. Puech, C. Estournès, A. Peigney, W. Bacsa, C. Laurent, The preparation of carbon nanotube (CNT)/copper composites and the effect of the number of CNT walls on their hardness, friction and wear properties, *Carbon* N. Y. 58 (2013) 185–197, <https://doi.org/10.1016/j.carbon.2013.02.049>.
- [41] A. Saboori, M. Pavese, C. Badini, P. Fino, A novel approach to enhance the mechanical strength and electrical and thermal conductivity of Cu-gnp nanocomposites, *Metall. Mater. Trans. A Phys. Metall. Mater. Sci.* 49 (2018) 333–345, <https://doi.org/10.1007/s11661-017-4409-y>.
- [42] A.K. Shukla, N. Nayan, S.V.S.N. Murty, S.C. Sharma, P. Chandran, S.R. Bakshi, K.M. George, Processing of copper-carbon nanotube composites by vacuum hot pressing technique, *Mater. Sci. Eng.* 560 (2013) 365–371, <https://doi.org/10.1016/j.msea.2012.09.080>.
- [43] L. Wang, Y. Cui, B. Li, S. Yang, R. Li, Z. Liu, R. Vajtai, W. Fei, High apparent strengthening efficiency for reduced graphene oxide in copper matrix composites produced by molecule-lever mixing and high-shear mixing, *RSC Adv.* 5 (2015) 51193–51200, <https://doi.org/10.1039/c5ra04782j>.
- [44] K. Chu, F. Wang, X. hu Wang, D. Jian Huang, Anisotropic mechanical properties of graphene/copper composites with aligned graphene, *Mater. Sci. Eng.* 713 (2018) 269–277, <https://doi.org/10.1016/j.msea.2017.12.080>.
- [45] P. Hidalgo-Manrique, X. Lei, R. Xu, M. Zhou, I.A. Kinloch, R.J. Young, Copper/graphene composites: a review, *J. Mater. Sci.* 54 (2019) 12236–12289, <https://doi.org/10.1007/s10853-019-03703-5>.
- [46] C. Subramaniam, Y. Yasuda, S. Takeya, S. Ata, A. Nishizawa, D. Futaba, T. Yamada, K. Hata, Carbon nanotube-copper exhibiting metal-like thermal conductivity and silicon-like thermal expansion for efficient cooling of electronics, *Nanoscale* 6 (2014) 2669–2674, <https://doi.org/10.1039/c3nr05290g>.
- [47] S. Arai, M. Endo, Various carbon nanofiber-copper composite films prepared by electrodeposition, *Electrochim. Commun.* 7 (2005) 19–22, <https://doi.org/10.1016/j.elecom.2004.10.008>.
- [48] S. Arai, M. Endo, Carbon nanofiber-copper composites fabricated by electroplating, *Electrochim. Solid State Lett.* 7 (2004) C25, <https://doi.org/10.1149/1.1644354>.
- [49] P.M. Hannula, S. Pletincx, D. Janas, K. Yliniemi, A. Hubin, M. Lundström, Controlling the deposition of silver and bimetallic silver/copper particles onto a carbon nanotube film by electrodeposition-redox replacement, *Surf. Coating. Technol.* 374 (2019) 305–316, <https://doi.org/10.1016/j.surfcoat.2019.05.085>.
- [50] M. Mecklenburg, A. Schuchardt, Y.K. Mishra, S. Kaps, R. Adelung, A. Lotnyk, L. Kienle, K. Schulte, Aerographite: ultra lightweight, flexible nanowall, carbon microtube material with outstanding mechanical performance, *Adv. Mater.* 24 (2012) 3486–3490, <https://doi.org/10.1002/adma.201200491>.
- [51] F. Schütt, S. Signetti, H. Krüger, S. Röder, D. Smazna, S. Kaps, S.N. Gorb, Y.K. Mishra, N.M. Pugno, R. Adelung, Hierarchical self-entangled carbon nanotube tube networks, *Nat. Commun.* 8 (2017) 1, <https://doi.org/10.1038/s41467-017-01324-7>.
- [52] R. Yuksel, O. Buyukcakir, P.K. Panda, S.H. Lee, Y. Jiang, D. Singh, S. Hansen, R. Adelung, Y.K. Mishra, R. Ahuja, R.S. Ruoff, Necklace-like nitrogen-doped tubular carbon 3D frameworks for electrochemical energy storage, *Adv. Funct. Mater.* 30 (2020) 1909725, <https://doi.org/10.1002/adfm.201909725>.
- [53] D. Janas, G. Stando, Unexpectedly strong hydrophilic character of free-standing thin films from carbon nanotubes, *Sci. Rep.* 7 (2017) 12274, <https://doi.org/10.1038/s41598-017-12443-y>.
- [54] B. Kumaneck, G. Stando, P.S. Wróbel, M. Krzywiecki, D. Janas, Thermoelectric properties of composite films from multi-walled carbon nanotubes and ethyl cellulose doped with heteroatoms, *Synth. Met.* 257 (2019) 116190, <https://doi.org/10.1016/j.synthmet.2019.116190>.
- [55] B. Kumaneck, T. Wasiak, G. Stando, P. Stando, D. Łukowiec, D. Janas, Simple method to improve electrical conductivity of films made from single-walled carbon nanotubes, *Nanomaterials* 9 (2019), <https://doi.org/10.3390/nano9081113>.
- [56] D. Janas, M. Rdest, K.K.K. Koziol, Free-standing films from chirality-controlled carbon nanotubes, *Mater. Des.* 121 (2017) 119–125, <https://doi.org/10.1016/j.matdes.2017.02.062>.
- [57] K.A. Worsley, I. Kalinina, E. Bekyarova, R.C. Haddon, Functionalization and dissolution of nitric acid treated single-walled carbon nanotubes, *J. Am. Chem. Soc.* 131 (2009) 18153–18158, <https://doi.org/10.1021/ja906267g>.
- [58] A. Castan, S. Forel, F. Fossard, J. Defiliet, A. Ghedjatti, D. Levshov, W. Wenseleers, S. Cambré, A. Loiseau, Assessing the reliability of the Raman peak counting method for the characterization of SWCNT diameter distributions: a cross-characterization with TEM, *Carbon* N. Y. (2020), <https://doi.org/10.1016/j.carbon.2020.09.012>.
- [59] A. Augustin, K. Rajendra Udupa, K. Udaya Bhat, Effect of coating current density on the wettability of electrodeposited copper thin film on aluminum substrate, *Perspect. Sci.* 8 (2016) 472–474, <https://doi.org/10.1016/j.pisc.2016.06.003>.
- [60] C.-W. Liu, J.-C. Tsao, M.-S. Tsai, Y.-L. Wang, Effects of wetting ability of plating electrolyte on Cu seed layer for electroplated copper film, *J. Vac. Sci. Technol. A Vacuum, Surfaces, Film.* 22 (2004) 2315–2320, <https://doi.org/10.1116/1.1795831>.
- [61] G. Stando, D. Łukawski, F. Lisiecki, D. Janas, Intrinsic hydrophilic character of carbon nanotube networks, *Appl. Surf. Sci.* 463 (2019), <https://doi.org/10.1016/j.apsusc.2018.08.206>.
- [62] H. Liu, J. Zhai, L. Jiang, Wetting and anti-wetting on aligned carbon nanotube films, *Soft Matter* 2 (2006) 811–821, <https://doi.org/10.1039/b606654b>.
- [63] J. Wang, Y. Wu, Y. Cao, G. Li, Y. Liao, Influence of surface roughness on contact angle hysteresis and spreading work, *Colloid Polym. Sci.* 298 (2020) 1107–1112, <https://doi.org/10.1007/s00396-020-04680-x>.
- [64] B. Kumaneck, G. Stando, P.S. Wróbel, D. Janas, Impact of synthesis parameters of multi-walled carbon nanotubes on their thermoelectric properties, *Materials (Basel)* 12 (2019), <https://doi.org/10.3390/ma12213567>.
- [65] P.R. Bandaru, Electrical properties and applications of carbon nanotube structures, *J. Nanosci. Nanotechnol.* 7 (2007) 1239–1267, <https://doi.org/10.1166/jnn.2007.307>.
- [66] P.M. Hannula, J. Aromaa, B.P. Wilson, D. Janas, K. Koziol, O. Forsén, M. Lundström, Observations of copper deposition on functionalized carbon nanotube films, *Electrochim. Acta* 232 (2017) 495–504, <https://doi.org/10.1016/j.electacta.2017.03.006>.